Kinetic Isotope Effects for Electron-Transfer Pathways in the Oxidative C−H Activation of Hydrocarbons

T. M. Bockman, S. M. Hubig, and J. K. Kochi*

Contribution from the Chemistry Department, University of Houston, Houston Texas 77204-5641

Received December 12, 1997

Abstract: Fast hydrogen atom transfers from various methylbenzenes (ArH) to photoactivated quinones **Q*** show primary kinetic isotope effects k(H)/k(D) of 2.4−5.6. The quantitative effects of added inert salt on the kinetics and on the yields of the intermediate cation radical $ArH^{+\bullet}$ demonstrate that hydrogen transfer proceeds via a two-step sequence involving an initial electron transfer to form the ion-radical pair [$ArH^{+\bullet}$, $Q^{-\bullet}$] which subsequently undergoes proton transfer according to the electron-transfer mechanism in Scheme 1.

Introduction

Facile carbon−hydrogen bond activation is critical to the synthetically important oxidative functionalizations of toluene and related hydrocarbons (ArH) to produce topical benzaldehydes, benzoic acids, and various benzyl derivatives with different ($1 - \epsilon$) organic and inorganic oxidants.[1,2] However, there is a recurring mechanistic ambiguity as to whether the initial C−H scission occurs (a) in a single step involving direct hydrogen-atom transfer[3] or (b) via prior electron transfer followed by proton transfer.[4,5] Deuterium labeling[8] has been used to address this important mechanistic question, and the observation of H(D) isotope effects on the kinetics of oxidation has been taken as conclusive evidence for the one-step formulation.[9] However, we now demonstrate that such a simple conclusion is incorrect and that (primary) deuterium isotope effects of appreciable magnitude are perfectly consistent with an electron-transfer mechanism for oxidative C−H bond activation.

Chart 1

Polymethylbenzene Donors (ArH)

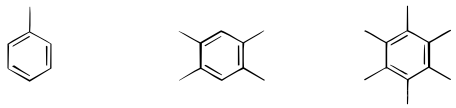

	TOL	DUR	HMB	
E^0_{ox}	2.40	1.84	1.62	V vs SCE

Quinone Acceptors (Q*)

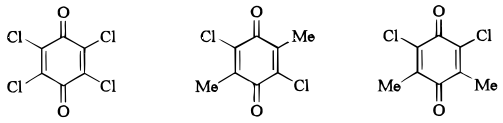

	CA	CX	CX'	
E^*_{red}	2.15	1.76	1.76	V vs SCE

Since quinones are effective dehydrogenation reagents as well as electron acceptors,[2a,10] we will focus our studies on the use of laser-activated quinones **Q*** with the enhanced reduction potentials (E^*_{red}) in Chart 1. Time-resolved absorption spectroscopy then allows the direct observation of all the short-lived intermediates involved in the diffusional interaction of **Q*** with the various methylbenzene donors (ArH with oxidation potentials E^0_{ox}) in Chart 1.

Results and Discussion

I. Spontaneous Activation of Quinone and Facile Hydrogen Transfer from Methylbenzenes. The photoactivation of quinone is spontaneously effected in dichloromethane by a 25-

(1) (a) Wiberg, K. B.; Evans, R. J. *Tetrahedron* **1960**, *8*, 313. (b) Hartford, W. H.; Darrin, M. *Chem. Rev.* **1958**, *58*, 1. (c) Onopchenko, A.; Schulz, J. G. D.; Seekircher, R. *J. Org. Chem.* **1972**, *37*, 1414. (d) Heiba, E. I.; Dessau, R. M.; Koehl Jr., W. J. *J. Am. Chem. Soc.* **1968**, *90*, 1082. (e) For a review on oxidations by metal complexes, see: Mijs, W. J.; de Jonge, C. R. H. I. *Organic Syntheses by Oxidation with Metal Compounds*; Plenum: New York, 1986.

(2) (a) Becker, H.-D. In *The Chemistry of the Quinone Compounds*, Part 1; Patai, S., Ed.; Wiley: New York, 1974; p 335. (b) Dauben, H. J., Jr.; Gedecki, F. A.; Harmon, K. M.; Pearson, D. L. *J. Am. Chem. Soc.* **1957**, *79*, 4557. (c) Longone, D. T.; Smith, G. L. *Tetrahedron Lett.* **1962**, 205. (d) Lee, I. S. H.; Jeong, E. H.; Kreevoy, M. M. *J. Am. Chem. Soc.* **1997**, *119*, 2722.

(3) (a) Wagner, P. J.; Truman, R. J.; Puchalski, A. E.; Wake, R. *J. Am. Chem. Soc.* **1986**, *108*, 7727. (b) Wagner, P. J.; Thomas, M. J.; Puchalski, A. E. *J. Am. Chem. Soc.* **1986**, *108*, 7739.

(4) (a) Traylor, T. G.; Nakano, T.; Miksztal, A. R.; Dunlap, B. E. *J. Am. Chem. Soc.* **1987**, *109*, 3625. (b) Jones, G., II; Mouli, N. *J. Phys. Chem.* **1988**, *92*, 7174. (c) Wagner, P. J. *Top. Curr. Chem.* **1976**, *66*, 1.

(5) The initial electron-transfer step in case (b) is generally reversible, so the latter case represents a classic example of a preequilibrium.[6] Unambiguous proof of preequilibria is a challenging experimental task, which is not readily accomplished by conventional kinetic measurements. Instead, additional approaches such as temperature studies, interception of precursors, and direct observation of the complete reaction sequence by time-resolved spectroscopic techniques must be brought to bear.[7]

(6) Bunnett, J. F. In *Investigation of Rates and Mechanisms of Reactions, Part 1*; Bernasconi, C. F., Ed.; Wiley: New York, 1986; p 268 f.

(7) (a) Baggott, J. E. In *Photoinduced Electron Transfer*; Fox, M. A., Chanon, M., Eds.; Elsevier: New York; 1988, Part B, p 385. (b) Strehlow, H.; Knoche, W. *Fundamentals of Chemical Relaxation*; Verlag Chemie: New York, 1977.

(8) (a) Carlson, B. W.; Miller, L. L. *J. Am. Chem. Soc.* **1985**, *107*, 479. (b) Pajak, J.; Brower, K. R. *J. Org. Chem.* **1985**, *50*, 2210. (c) Dinktürk, S.; Ridd, J. H. *J. Chem. Soc., Perkin Trans. 2* **1982**, 1961.

(9) (a) Gardner, K. A.; Mayer, J. M. *Science* **1995**, *269*, 1849. (b) Gardner, K. A.; Kuenert, L. A.; Mayer, J. M. *Inorg. Chem.* **1997**, *36*, 2069. (c) Höfler, C.; Rüchardt, C. *Liebigs Ann.* **1996**, 183.

(10) Rathore, R.; Hubig, S. M.; Kochi, J. K. *J. Am. Chem. Soc.* **1997**, *119*, 11468.

S0002-7863(97)04205-4 CCC: $15.00
Published on Web 03/12/1998

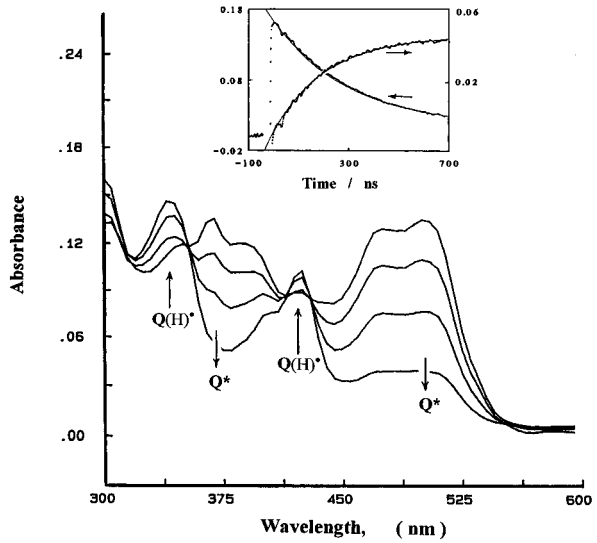

Figure 1. Spectral changes attendant upon hydrogen transfer from 0.005 M durene to **Q*** generated by the 355-nm excitation of 0.002 M **Q**(**CX**) in dichloromethane at 23 °C. Inset shows the digital fit (smooth line) of the **Q*** decay and **Q**(**H**)• growth to first-order kinetics with $k_{obs} = 3.6$ and $4.3(\pm 0.5) \times 10^6$ s^{-1} as followed at 500 and 335 nm, respectively.

ps laser pulse at 355 nm to yield the characteristic spectrum of **Q*** with unit efficiency.[10,11] The subsequent first-order decay of **Q*** in the presence of ArH is accompanied by the simultaneous appearance of the reduced **Q**(H)•[12] and the benzylic radical (Ar•)[13] in equimolar amounts. As such, hydrogen transfer according to eq 1 is conveniently monitored by the temporal evolution of the diagnostic absorption spectra of both **Q*** and **Q**(H)• previously reported.[14]

$$\mathbf{Q}^* + \mathrm{ArH} \xrightarrow{k_2} \mathbf{Q}(\mathrm{H})^\bullet + \mathrm{Ar}^\bullet \qquad (1)$$

Hydrogen transfer from durene as a typical ArH (in excess) is illustrated in Figure 1 by the monotonic disappearance of **Q***, and it is accompanied by the concomitant production of the reduced quinone radical **Q**(H)•.[14] The rate of hydrogen transfer is conveniently monitored by the temporal evolution of the diagnostic spectra of **Q*** and **Q**(H)•.[14] In Figure 1, the spectral band of **Q*** with $\lambda_{max} = 500$ nm decreases smoothly as the sharp band of the reduced quinone **Q**(H)• at $\lambda_{max} = 435$ nm increases. The assignment of the 435-nm band to **Q**(H)• is confirmed by the simultaneous appearance of its UV band at 360 nm.[10] The isosbestic points at 370, 400, and 440 nm indicate that the transformation occurs uniformly,[15] and the decay of **Q*** and the rise of **Q**(H)• both follow first-order kinetics

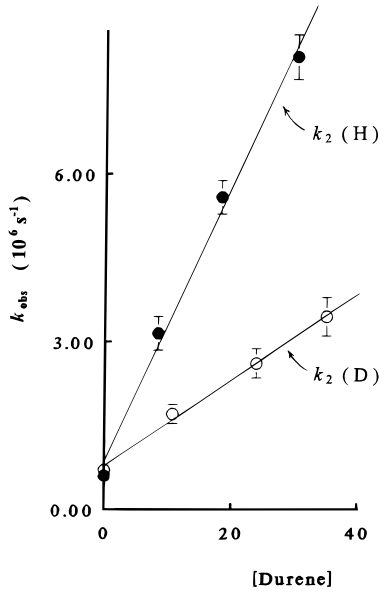

Figure 2. Pseudo-first-order plots of k_{obs} with durene (●) and durene-d_{14} (○) in dichloromethane, as described in Figure 1.

Table 1. Kinetic Isotope Effect for Hydrogen Transfer from Methylbenzenes to **Q*** [a]

Q/ArH[b]	k_2(H) [M^{-1} s^{-1}]	k_2(D) [M^{-1} s^{-1}]	k_2(H)/k_2(D)	$(k^H/k^D)_{PT}$
CX/DUR	2.4×10^8	7.9×10^7	3.0 (3.3)	2.4
CX′/DUR	3.7×10^8	1.3×10^8	2.8 (*c*)	5.6
CX/HMB	*d*	*d*	*d* (3.1)	4.4
CA/TOL	1.8×10^7	6.8×10^6	2.6 (1.6)	*e*
CA/DUR	1.2×10^{10}	7.2×10^9	1.7 (2.4)	2.8
CA/BIP	4.2×10^8	4.3×10^8	0.99	*f*

[a] Measured as bimolecular rate constants k_2 for **Q*** and ArH upon the 355-nm excitation (15 mJ per pulse) of 0.005 M **Q** and various concentrations of ArH in dichloromethane as described in the text. [b] Quinone and methylbenzene identified in Chart 1. [c] Not measured. [d] Measured only under diffusion-free conditions (as described in the Experimental Section). [e] No free ions observed. [f] No hydrogen transfer observed from biphenyl (BIP), as described in ref 22.

with the same rate constant (k_{obs}) as shown by the digital fits in the inset to Figure 1 to confirm a simple kinetic formulation. The linear variation in k_{obs} as a function of ArH concentration is shown in Figure 2, and the rate constant for the bimolecular reaction in eq 1 is simply given by the slope of this pseudo-first-order plot. [See the Experimental Section for details of this analysis.] The values of the bimolecular rate constants (k_2) for various combinations of methylarenes and quinones are compiled in Table 1.

II. Kinetic Isotope Effect for Hydrogen Transfer. The effect of isotopic substitution is readily evaluated by comparing the bimolecular rate constant k_2(D) for perdeuterated ArD with the rate constant k_2(H) for its protiated parent. For example, Figure 2 shows the distinctly slower rates which govern the abstraction of deuterium from durene-d_{14}, and the isotope effect on k_2 is readily evaluated from the slope of the kinetics plot. The isotope effects (k_2^H/k_2^D) for various methylbenzenes are listed in Table 1 (fourth column). It is noteworthy that the kinetic isotope effects require the presence of a benzylic hydrogen, since there is no difference in the rates with which **Q*** is reduced by biphenyl or biphenyl-d_{10} (entry 6).[22]

III. Interception of the Transient Intermediates by Added Salt. Let us now address the question as to whether the observed kinetic isotope effects in Table 1 rule out an electron-transfer mechanism. To probe the possibility of such an alternative pathway, we employ inert salt to intercept the ion-

(11) Hubig, S. M.; Bockman, T. M.; Kochi, J. K. *J. Am. Chem. Soc.* **1997**, *119*, 2926.

(12) (a) Kobashi, H.; Funabashi, M.-A.; Kondo, T.; Morita, T.; Okada, T.; Mataga, N. *Bull. Chem. Soc. Jpn.* **1984**, *57*, 3557. (b) Kobashi, H.; Okada, T.; Mataga, N. *Bull. Chem. Soc. Jpn.* **1986**, *59*, 1975. (c) Jones, G., II; Haney, W. A.; Phan, X. T. *J. Am. Chem. Soc.* **1988**, *110*, 1922.

(13) (a) Christensen, H. C.; Sehested, K.; Hart, E. J. *J. Phys. Chem.* **1973**, *77*, 983. (b) The absorption of the trimethylbenzyl radical Ar• at λ_{max} = 310 nm is obscured by the overlapping absorptions of the quinone radical and other long-lived products of the hydrogen transfer.

(14) (a) For the quinone transients, the diagnostic absorption maxima are as follows: **CA*** (510 nm, $\epsilon = 7600$ M^{-1} cm^{-1}), **CA**(H)• (435 nm, $\epsilon = 7700$ M^{-1} cm^{-1}), **CA**$^{-\bullet}$ (450 nm, $\epsilon = 9600$ M^{-1} cm^{-1}), **CX*** (500 nm, $\epsilon = 5300$ M^{-1} cm^{-1}), **CX**(H)• (340 nm, $\epsilon = 5300$ M^{-1} cm^{-1}), and **CX**$^{-\bullet}$ (430 nm, $\epsilon = 6800$ M^{-1} cm^{-1}) as described in ref 10. (b) Note that the decay rate of **Q*** in the absence of ArH is much slower ($k_{obs} < 10^5$ s^{-1}) than the rates of hydrogen transfer in eq 1. See ref 10.

(15) Moore, J. W.; Pearson, R. G. *Kinetics and Mechanism*, 3rd ed.; Wiley: New York, 1981; p 49.

SALT EFFECTS

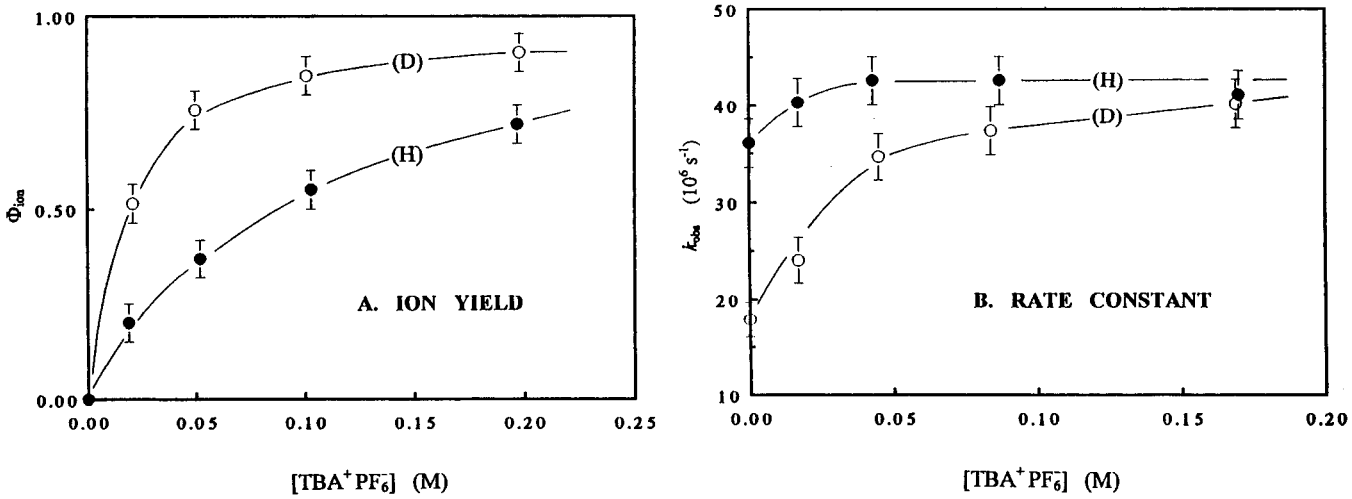

Figure 3. Salt effects with $TBA^+PF_6^-$ on (A) the ion yields of $ArH^{+\bullet}$ and (B) the first-order rate constant for the reaction of **Q***(**CX**) with HMB (●) and HMB-d_{18} (○) in dichloromethane by the procedure described in Figure 1.

radical pair intermediate prior to proton transfer in the following way. Upon the addition of the neutral electrolyte, tetra-*n*-butylammonium hexafluorophosphate (TBA^+ PF_6^-), the transient spectrum of **Q**(H)$^\bullet$ in Figure 1 is replaced by that of the anion radical $\mathbf{Q}^{-\bullet}$. Most importantly, the characteristic spectral band of the arene cation radical, $ArH^{+\bullet}$,[16] which is not present in the absence of TBA^+ PF_6^-, now becomes a dominant feature. For example, in the presence of TBA^+ PF_6^-, a dichloromethane solution of hexamethylbenzene and quinone produces high yields of the quinone anion radical (with $\lambda_{max} = 330$ and 430 nm) and the methylbenzene cation radical (with $\lambda_{max} = 495$ nm) in equimolar amounts. In other words, added salt drastically alters the original spectral transformation from **Q*** to the radical **Q**(H)$^\bullet$ in eq 1 to one that generates the anion $\mathbf{Q}^{-\bullet}$, *i.e.*

$$\mathbf{Q}^* + \mathrm{ArH} \xrightarrow{\mathrm{TBA^+PF_6^-}} \mathbf{Q}^{-\bullet} + \mathrm{ArH}^{+\bullet} \qquad (2)$$

The quantitative effects of added salt on the yields of the ions $\mathbf{Q}^{-\bullet}$ and $ArH^{+\bullet}$ in eq 2 are evaluated in Table 2 as the quantum yields Φ_{ion} by using benzophenone as the transient actinometer[10,17] (see the Experimental Section). Figure 3A demonstrates the yield of $ArH^{+\bullet}$ to increase monotonically with increasing salt concentration[18] in accord with the progressive replacement of **Q**(H)$^\bullet$ with $\mathbf{Q}^{-\bullet}$ in the transient spectra.

Table 2. Effect of Added Salt on the Quantum Yield of $ArH^{+\bullet}$ and the Pseudo-First-Order Rate Constant

	[salt] (M)[c]							
	Φ_{ion}[a]				k_{obs}[b] [10^7M^{-1} s^{-1}]			
Q/ArH[d]	0.02	0.05	0.10	0.20	0	0.05	0.10	0.20
CX/HMB	0.20	0.37	0.55	0.72	3.6	4.2	4.3	4.1
CX/HMB-d_{18}	0.52	0.76	0.84	0.90	1.7	3.5	3.7	4.0
CA/DUR	0.72	0.78	0.88	0.96				
CA/DUR-d_{14}	0.84	1.00	1.00	1.00				
CX/DUR	0.10	0.17	0.26	0.39	1.7	2.3	2.8	3.3
CX/DUR-d_{14}	0.17	0.22	0.39	0.57	0.6	0.9	1.2	1.6
CA/HMB	0.57	0.78	0.87	1.00				
CA/HMB-d_{18}	0.85	0.99	1.00	1.00				

[a] Yield of cation radicals $ArH^{+\bullet}$ as determined by transient actinometry, see text. [b] Observed (pseudo-first-order) rate constant (±0.05) for the decay of excited quinone (**Q***) upon the 355-nm excitation (15 mJ per pulse) of 0.005M **Q** and 0.008 M hexamethylbenzene (HMB) or 0.12 M durene (DUR) in dichloromethane at 23 °C. [c] Tetrabutylammonium hexafluorophosphate (see also ref 18 and the Experimental Section). $\Phi_{ion} = 0$ in the absence of salt with all **Q**/ArH combinations. [d] Quinone and methylbenzene identified in Chart 1.

In contrast to the strong effect of added salt on the product yields, the effect on their *rates of formation* is insignificant.[19] Figure 3B shows the rate constant for hydrogen transfer from hexamethylbenzene to **Q*** (filled circles) to be essentially unaffected by the addition of TBA^+ PF_6^-. Similarly, there is only a minor effect of added salt on the kinetics (k_{obs}) of the hydrogen abstraction from durene in Table 2.

IV. Electron-Transfer Pathway for Hydrogen Transfer. The foregoing effect of an additive in eq 2 (to completely transform the reaction products while leaving the overall rate essentially unaffected) is incompatible with a one-step mechanism for direct hydrogen transfer (eq 1), since it demands the existence of another intermediate.[6] Furthermore, the particular effect of added *salt* implies that this intermediate must be an ionic species. From the known behavior of quinones in their excited states to readily oxidize electron-rich organic donors to their cation radicals,[10] we identify the ionic intermediate as the ion pair [$\mathbf{Q}^{-\bullet}$, $ArH^{+\bullet}$] which is known to be readily intercepted

(16) For the methylbenzene transients, the diagnostic absorption maxima are as follows: $HMB^{+\bullet}$ (495 nm; $\epsilon = 2500$ M^{-1} cm^{-1}), $DUR^{+\bullet}$ (480 nm; $\epsilon = 2400$ M^{-1} cm^{-1}), and TOL (420 nm). See (a) Bockman, T. M.; Karpinski, Z. J.; Sankararaman, S.; Kochi, J. K. *J. Am. Chem. Soc.* **1992**, *114*, 1970. (b) Sehested, K.; Holcman, J.; Hart, E. J. *J. Phys. Chem.* **1977**, *81*, 1363.

(17) Hurley, J. K.; Sinai, N.; Linschitz, H. *Photochem. Photobiol.* **1983**, *38*, 9.

(18) Aggregation of TBA^+ PF_6^- is not significant in this concentration range. See: Sigvartsen, T.; Gestblom, B.; Noreland, E.; Songstad, J. *Acta Chem. Scand.* **1989**, *43*, 103 (compare the results for $TBA^+PF_6^-$, $TBA^+ClO_4^-$, and $PPN^+PF_6^-$ in the Experimental Section).

(19) (a) Gordon, J. E. *The Organic Chemistry of Electrolyte Solutions*; Wiley: New York, 1975; p 99 f. See also: (b) Masnovi, J. M.; Kochi, J. K. *J. Am. Chem. Soc.* **1985**, *107*, 7880. (c) Yabe, T.; Kochi, J. K. *J. Am. Chem. Soc.* **1992**, *114*, 4491.

(20) Note that any subsequent proton transfer for the separated ion radicals occurs by second-order kinetics and is therefore negligibly slow.

(21) (a) Schlesener, C. J.; Amatore, C.; Kochi, J. K. *J. Am. Chem. Soc.* **1984**, *106*, 7472. (b) Masnovi, J. M.; Sankararaman, S.; Kochi, J. K. *J. Am. Chem. Soc.* **1989**, *111*, 2263.

(22) Kinetic isotope effects on simple electron transfers, without a follow-up proton-transfer step, are small ($k_{ET}^H/k_{ET}^D \leq 1.3$). See: (a) Pal, H.; Nagasawa, Y.; Tominaga, K.; Yoshihara, K. *J. Phys. Chem.* **1996**, *100*, 11964. (b) Doolen, R.; Simon, J. D. *J. Am. Chem. Soc.* **1994**, *116*, 1155 (compare the results with biphenyl (entry 6 in Table 1)).

by added salt.[19]

$$[ArH^{+\bullet}, \mathbf{Q}^{-\bullet}] + TBA^{+}, PF_6^{-} \overset{k_S}{\rightleftharpoons} TBA^{+}, \mathbf{Q}^{-\bullet} + ArH^{+\bullet}, PF_6^{-} \quad (3)$$

We therefore conclude that the critical step to form $\mathbf{Q}(H)^{\bullet}$ and $Ar^{\bullet}$ as the products of hydrogen transfer is to be identified as proton transfer (k_{PT}) from $ArH^{+\bullet}$ to $\mathbf{Q}^{-\bullet}$ within the contact ion pair in eq 4.[20]

$$\mathbf{Q}^{*} + ArH \xrightarrow{k_{ET}} [\mathbf{Q}^{-\bullet}, ArH^{+\bullet}] \xrightarrow{k_{PT}} \mathbf{Q}(H)^{\bullet} + Ar^{\bullet} \quad (4)$$

The pathway in eq 4 might appear to be incompatible with the observed isotope effects in Table 1, since the initial electron-transfer step is not expected to show an appreciable isotope effect. To resolve this paradox, let us consider the cumulative effect of added salt on the kinetic isotope effect. In the absence of any salt, $\mathbf{Q}^{*}$ reacts appreciably slower with the perdeuterated methylarenes, and the difference is reflected in the kinetic isotope effect (3.1 for HMB) which is more or less that for deprotonation of various $ArH^{+\bullet}$ by pyridine bases.[21] Most strikingly, the progressive addition of $TBA^{+}PF_6^{-}$ causes a corresponding diminution in the deuterium isotope effects (compare the open circles relative to the filled circles in Figure 3B), such that at the (highest) salt concentration of 0.2 M the isotope effect completely vanishes in Figure 3B! Equally striking is the concomitant increase in the ion yields of $ArH^{+\bullet}$ with increasing salt concentration in Figure 3A to establish the salt-induced competition between ion-pair separation (k_S) and proton transfer (k_{PT}), *i.e.*

$$ArH^{+\bullet} + \mathbf{Q}^{-\bullet} \xleftarrow{k_S} [ArH^{+\bullet}, \mathbf{Q}^{-\bullet}] \xrightarrow{k_{PT}} Ar^{\bullet} + \mathbf{Q}(H)^{\bullet} \quad (5)$$

Such a formulation emphasizes the effect of added salt on the kinetic isotope effect to parallel its effect on the ion yield, which is consistently greater for the deuterated analogue (ArD). The difference, however, diminishes with increasing salt concentrations, as the yield of cation radical approaches unity for both isotopomers.

Salt effects in eq 5 predict the ion-pair separation in eq 2 to be complete at sufficiently high salt concentrations, and this will lead to the loss of the kinetic isotope effect. Thus the difference in reactivity between ArH and ArD in Table 1 must stem entirely from the proton-transfer step (k_{PT}) in eq 4.[22] Since the overall decay rate of $\mathbf{Q}^{*}$ *is* affected by isotopic substitution, the kinetics of this follow-up step must feed back onto the initial electron-transfer step. For this condition to hold, electron transfer must be reversible. As such, the inclusion of the salt-induced separation and reverse electron transfer leads to the modification of the ET mechanism in eq 4 to that shown in Scheme 1.

In this scheme, the isotope effect on the proton transfer (k_{PT}) is "diluted" by the competing ion separation (k_S) as well as the reversible electron transfer (k_{-ET}). Thus, the isotope effect decreases as the free-ion yields increase, and such an inverse relationship is verified in Figure 3. For the competition in Scheme 1, the ion yield is readily formulated as $\Phi_{ion} = k_S[salt]/(k_{PT} + k_S[salt])$,[23] which leads to the linearized correlation $\Phi_{ion}^{-1} = 1 + (k_{PT}/k_S)\,[salt]^{-1}$, and this is confirmed in Figure 4 by the linear plot of the reciprocal ion yields (Φ_{ion}^{-1}) versus the reciprocal salt concentration $[salt]^{-1}$. Most notably,

(23) The bimolecular formulation of the salt effect in Scheme 1 is likely to be an oversimplification, since it assumes that added salt reacts as a simple molecular species and does not take into account the behavior of the separated ions.

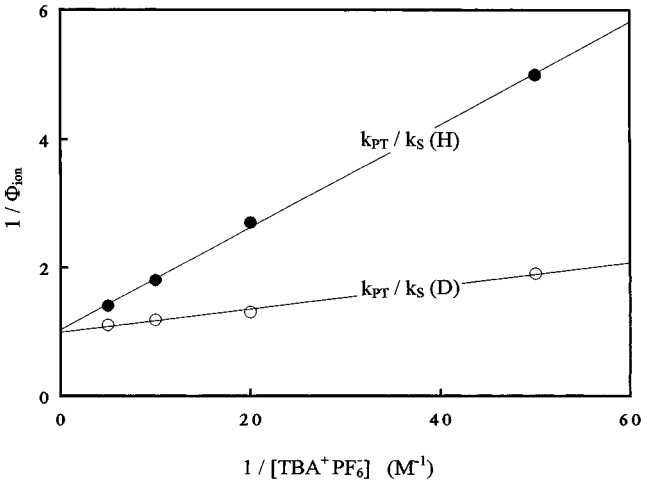

Figure 4. Linear correlation of the competition between proton transfer (k_{PT}) and ion separation (k_S) as derived from the salt effect on $ArH^{+\bullet}$ yields in Figure 3A according to the mechanism in Scheme 1.

Scheme 1

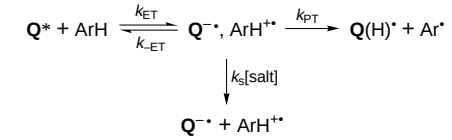

the theoretical intercept of $\Phi_{ion} = 1.0$ solidifies this prediction, and the slope (k_{PT}/k_S) leads to the isotope effect for proton transfer ($k^H/k^D)_{PT}$ listed in the last column in Table 1.[24]

Summary and Conclusions

We have unambiguously demonstrated that substantial kinetic isotope effects are observed for the hydrogen transfer in eq 1, even when it proceeds via a two-step sequence involving reversible electron transfer followed by proton transfer according to Scheme 1. This mechanism is applicable to the oxidative C−H activation of most hydrocarbons which involve endergonic electron transfer ($\Delta G \geq 0$), so that reverse electron transfer (k_{-ET}) is competitive with proton transfer (k_{PT}). Although analogous electron-transfer formulations are applicable to a wide variety of other organic reactions,[25] their experimental verification (as elucidated herein) will be difficult, since the rapidity of the follow-up steps generally precludes the direct observation of the ion-radical pair. Indeed, time-resolved spectroscopy,

(24) If the ion-radical pair in Scheme 1 is assumed to be present in a dynamic steady-state concentration, the bimolecular rate constant, k_2, is given by $k_2 = k_{ET}(k_{PT} + k_S[salt])/(k_{-ET} + k_{PT} + k_S[salt])$. Two limiting cases arise from this equation. For case (i), $k_{PT} \gg k_{-ET} + k_S[salt]$, k_2 is simply given by k_{ET}. No kinetic isotope effect is expected in this case. For case (ii), $k_{-ET} \gg k_{PT} + k_S[salt]$, k_2 is given by $(k_{ET}/k_{-ET})(k_{PT} + k_S[salt])$. In this case, the kinetic isotope effect (in the absence of added salt) will be identical to that of the intrinsic proton transfer, i.e., $(k^H/k^D)_{PT}$ in Table 1. Thus the measured kinetic isotope effect on k_2 will fall between these extremes. (b) Digital simulation of the complete (complex) kinetics in Scheme 1, using the method of Weigert,[24c] leads to the same conclusion. (c) Weigert, F. *J. Comput. Chem.* **1987**, *11*, 273.

(25) The mechanistic ambiguity addressed in this study applies to other hydrogen-atom transfer reactions, as well as a wide variety of organic processes for which an initial electron-transfer process may be formulated. For H-atom transfers, see: (a) Patz, M.: Fukuzumi, S. *J. Phys. Org. Chem.* **1997**, *10*, 129. For other reactions, see: (b) Olah, G. A.; Malhotra, R.; Narang, S. C. *Nitration: Methods and Mechanism*; VCH: New York, 1989; p 166 f (nitration). (c) Baciocchi, E.; Galli, C. *J. Phys. Org. Chem.* **1995**, *8*, 563 (halogenation). (d) Tolbert, L. M.; Sun, X. J.; Ashby, E. C. *J. Am. Chem. Soc.* **1995**, *117*, 2681 (nucleophilic substitution). (e) Freilich, S. C.; Peters, K. S. *J. Am. Chem. Soc.* **1985**, *107*, 3819 (cycloaddition). (f) Lopez, L.; Troisi, L. *Tetrahedron Lett.* **1989**, *30*, 3097 (rearrangement of epoxides). For organometallic examples, see: (g) Astruc, D. *Electron Transfer and Radical Processes in Transition-Metal Chemistry*; VCH: New York, 1995.

combined with the efficacy of added salt, has provided us with a unique opportunity to intercept and quantify this elusive intermediate. More typically, the transient ion pair is unobservable, and we are left with a reaction that appears to proceed via a single (concerted) step.

Experimental Section

Materials. Chloranil, hexamethylbenzene, and durene in Chart 1 were obtained from Aldrich and purified by recrystallization from ethanol.[26] Toluene was distilled from sodium and benzophenone in an atmosphere of argon. Toluene-d_8 (Aldrich), durene-d_{14} (KOR Isotopes), hexamethylbenzene-d_{18} (MSD Isotopes), biphenyl-d_{10} (Aldrich), and tetra-*n*-butylammonium hexafluorophosphate and perchlorate (Aldrich) were used as received. Dichloromethane (reagent grade) was stirred over concentrated H_2SO_4, washed with aqueous $NaHCO_3$, and distilled serially from P_2O_5 and from CaH_2 under an argon atmosphere. The synthesis of 2,5-dichloroxyloquinone (CX) was described previously.[10] 2,6-Dichloroxyloquinone (CX′) was prepared as follows: 2,6-dimethyl-1,4-dimethoxybenzene (Aldrich) was chlorinated overnight with chlorine gas in carbon tetrachloride at room temperature, and 2,6-dichloro-3,5-dimethyl-1,4-dimethoxybenzene was obtained in 90% yield. Demethylation with BBr_3 in dichloromethane yielded the corresponding hydroquinone, which was subsequently oxidized with N_2O_4 to 2,6-dichloroxyloquinone (CX′) in 86% yield. The quinone was purified by recrystallization from ethanol.

Determination of the Bimolecular Rate Constants for Hydrogen Transfer. The laser-flash experiments were carried out using the third harmonic (355 nm) of a Q-switched Nd:YAG laser (10-ns fwhm) and a kinetic spectrometer described in detail elsewhere.[16a] **General Procedure.** Upon laser excitation of the quinone (5.0×10^{-3} M) in dichloromethane, the decay of the triplet quinone was observed at 500 nm in the presence of varying concentrations (10^{-3}−10^{-1} M) of polymethylbenzene. The transient decay was fitted to first-order kinetics, and the observed rate constants (k_{obs}) were plotted against the arene concentration. (A) The plot was linear for arene concentrations in the range of 10^{-3} to approximately 5×10^{-2} M, and the slope of these plots yielded the bimolecular rate constants (k_2) in Table 1. (B) The kinetics plots of the observed first-order rate constants versus the ArH concentrations did not remain linear at high [ArH] but approached a plateau value for concentrations greater than 3.0×10^{-1} M. This asymptotic behavior of the kinetics plots was diagnostic of a preequilibrium intermediate, which was previously identified as the encounter complex [**Q***, ArH] of the photoactivated quinone and the polymethylbenzene.[10] Thus the limiting values of k_{obs} at high [ArH] represented the intrinsic decay (electron-transfer) rate constant of the encounter complex. Since the encounter complex decayed after its diffusive formation from **Q*** and ArH, the limiting decay rate constants represented electron transfer in the absence of diffusion. The ratios of these rate constants for the protiated and deuterated polymethylbenzenes yielded the kinetic isotope effect under these diffusion-free conditions, and they are listed in Table 1 in parentheses.

Determination of the Quantum Yields for Ion-Radical Formation. The yields of the ion radicals in dichloromethane solutions containing varying amounts of added salt ($TBA^+ PF_6^-$) were determined by using benzophenone in benzene as the transient actinometer.[10,17] Thus, samples of the actinometer solution and the quinone/arene solution in dichloromethane containing 0.02, 0.05, 0.10, and 0.20 M salt with matching absorbances at 355 nm were excited with the 10-ns pulse of the Nd:YAG laser. The yields of the ion radicals were determined by quantitative comparison of the maximum absorbance of triplet benzophenone ($\epsilon_{530} = 7220$ M^{-1} cm^{-1})[17] with the maximum absorbance of the cation radical (e.g., $HMB^{+\bullet}$ and $DUR^{+\bullet}$, at 495 and 480 nm, respectively, both with $\epsilon = 2500$ M^{-1} cm^{-1}).[16] The observed salt effect for $TBA^+ PF_6^-$ was the same as that for two other salts, ($TBA^+ ClO_4^-$) and [$PPN^+ PF_6^-$], and values of Φ_{ion} for the three salts in the concentration range (i) 0.05, (ii) 0.10, and (iii) 0.20 M are given serially as follows: (i) 0.52, (0.52), [0.56]; (ii) 0.70 (0.70), [0.75]; (iii) 0.84, (0.85), [0.89] for **CX*** and HMB in dichloromethane at 23 °C.

Acknowledgment. We thank R. Rathore for providing the dichloroxyloquinones in Chart 1, and the National Science Foundation and the R. A. Welch Foundation for financial support.

JA974205S

(26) Perrin, D. D.; Armarego, W. L. F. *Purification of Laboratory Chemicals*, 3rd ed.; Pergamon: Oxford, 1988.